

Resist materials and processes for X-ray lithography

by David Seeger

A key component that is sometimes overlooked in X-ray lithography is the resist material. The lithographic properties of these materials are extremely important if one is to take advantage of the superior lithographic performance often observed in X-ray lithography. The properties of such materials may even be more important than in conventional optical lithography, since the feature sizes delineated by this lithographic technique are much smaller. A description of X-ray resists is presented which discusses both the chemistry and the lithographic properties of these materials. The characterization and stability of these processes are highlighted.

Introduction

In this paper, we initially describe X-ray lithographic processes from a materials perspective. The focus of the first section is on the absorption of X-rays in materials as well as description of the chemical processes that occur after the initial absorption. The chemistry of the types of materials used in X-ray lithography (XRL) is described, beginning with the classic diazoquinone novolak materials widely used in the semiconductor industry. This is

followed by a discussion of the chemistry of the newer class of chemically amplified resist systems.

A description is given of the lithographic aspects of X-ray resist processes under synchrotron radiation, and the process latitude of resist systems is outlined. An understanding of how changes in dissolution characteristics affect the lithographic properties of the resist is highlighted. Finally, we conclude by describing the extendibility of X-ray lithographic processes to dimensions for use in future technologies.

X-ray resist materials: Overview and chemistry

As with any lithography, the object in XRL is to pattern a semiconductor wafer with the desired design. This is typically done by using a photoresist material as a mask which is patterned during the lithographic step. This can be accomplished with either a positive-tone resist, which replicates the mask directly, or a negative-tone resist, which creates an image with the opposite tone (**Figure 1**).

From a materials point of view, XRL has leveraged the tremendous amount of work that has gone into the design of optical resist materials. Such materials are typically composed of a resin and a photo-labile component, either as a separate molecule or part of the resin itself. During the exposure step, the photo-labile material undergoes a chemical change. In conventional resist materials, this chemical change causes a solubility difference of the resist

©Copyright 1993 by International Business Machines Corporation. Copying in printed form for private use is permitted without payment of royalty provided that (1) each reproduction is done without alteration and (2) the *Journal* reference and IBM copyright notice are included on the first page. The title and abstract, but no other portions, of this paper may be copied or distributed royalty free without further permission by computer-based and other information-service systems. Permission to *republish* any other portion of this paper must be obtained from the Editor.

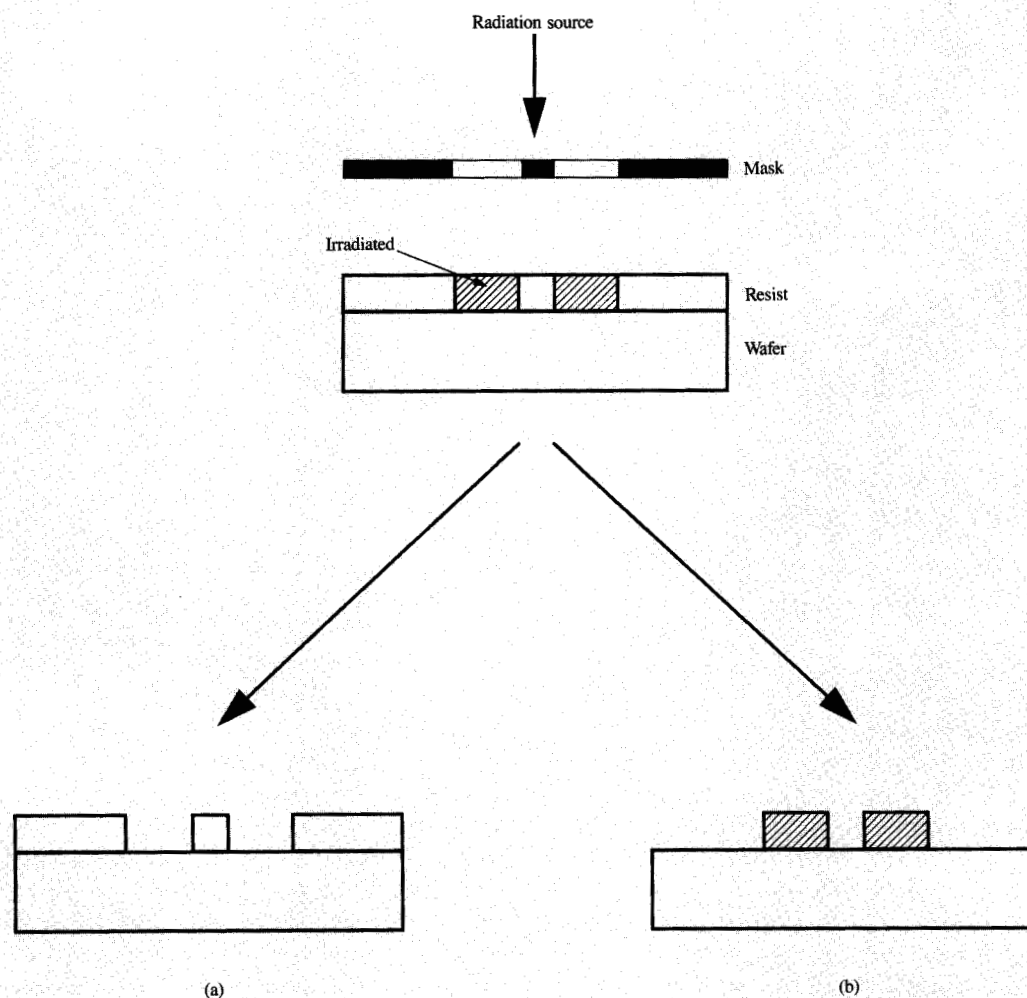


Figure 1

Schematic of (a) positive-tone and (b) negative-tone resist processing.

when it is placed in developer. This difference can be exploited during development to create a three-dimensional structure on the wafer.

Unique to X-ray lithography is the wavelength of irradiation used. A detailed description of how X-rays interact with matter can be found elsewhere [1]. The nature of this interaction depends strongly on the wavelength of incident irradiation and, for the purposes of this discussion, it is assumed that the irradiation wavelength is that found in synchrotron-based XRL. In this type of lithography, the radiation is typically in a wavelength band from 6–12 Å. At these wavelengths, organic materials are relatively transparent (~10% absorbed/ μm). Because of the high energy of incoming

photons, an absorbed photon ionizes a core electron within an atom. Therefore, in contrast to optical lithography, in XRL valence electrons have only a minimal effect on X-ray absorption, and one can think of a resist material as an array of atoms in which the types and nature of chemical bonds are relatively unimportant. This greatly simplifies determination of bulk absorption properties of materials. The absorption of a material is easily calculated by merely knowing the relative number of atoms in a material, the X-ray mass absorption coefficient for each atom, and the density of the material.

As mentioned above, the wavelength of the radiation is an important factor, since the absorption of atoms varies as a function of the energy of the photon. As an example,

carbon is almost three times more absorbent at 11.9 Å than at 8.34 Å. Since resist materials are primarily composed of carbon atoms, the resist is more absorbent at the longer wavelength.

For resists designed for XRL, studies have been focused on increasing the absorption of X-rays in materials by the incorporation of specific atoms [2]. Specifically, incorporation of halogens into polymers has been widely investigated because the halogens have relatively high X-ray cross sections. Some examples of these materials are halogenated methacrylate derivatives such as polydimethyltetrafluoro propyl methacrylate, poly-2-fluoro ethyl methacrylate, and poly-2-chloroethylmethacrylate [3]. These materials have shown improvements in sensitivity of 5–8× because of the improved X-ray absorption properties.

An understanding of the basic chemistry that occurs under X-ray irradiation is important if one is to make further improvements in X-ray resists. There are some studies in the literature which attempt to quantify differences in chemistry between different radiation sources. Differences between ionizing (e-beam, X-ray) and nonionizing (ultraviolet) radiation have been reported and are not unexpected [1]. There are reports indicating strong correlations between X-ray and e-beam resist sensitivities [4]. While there is a clear correlation in some cases, it is not clear that the mechanisms of photochemistry of these two radiations are the same. At least one published report [5] presents subtle but distinct differences between these two forms of irradiation of polymethyl methacrylate (PMMA).

Since diazoquinone novolak resist systems are widely used in the semiconductor industry, we evaluated the photochemistry of this type of material under synchrotron irradiation. These materials are composed of a novolak resin and the alpha diazoketone shown in Figure 2(a). We studied an IBM resist of this type, TNS [6], by Fourier transform infrared (FT-IR) spectroscopy. Resist materials were spin-coated onto KBr discs and exposed with varying levels of synchrotron radiation. FT-IR analyses of irradiated and unirradiated samples were done, and the results were compared to those for samples irradiated with ultraviolet light.

The chemistry of UV-irradiated samples has been well documented [7] and involves loss of the diazo group forming the corresponding carbene, as shown in Figure 2(a). This intermediate undergoes rapid Wolff rearrangement, forming a ring-contracted ketene which is hydrolyzed by reaction with residual water in the resin to form a carboxylic acid. It is the destruction of the diazo material (which is insoluble in basic developer and acts as a dissolution inhibitor) and formation of the carboxylic acid that create the dissolution differences between exposed and unexposed resist.

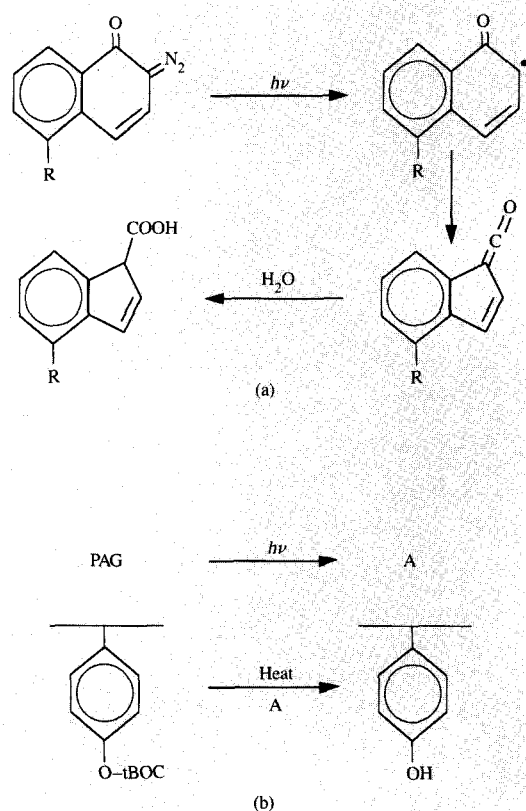


Figure 2

Schematic of the chemistry for (a) a diazoquinone novolak resist system and (b) a chemically amplified resist system. PAG is the photo-acid generator and A is a strong acid.

In our analysis, two peaks corresponding to the starting diazo compound [2115 cm^{-1} (diazo peak), 1600 cm^{-1} (carbonyl stretch from the diazo compound)] and one peak from the carboxylic acid photoproduct [1717 cm^{-1} (carboxylic carbonyl stretch)] were examined. After six seconds of UV irradiation, both peaks from the diazo compound decreased in relative intensity by 20% and the peak from the carboxylic product increased by 31%. After an additional 12 seconds of irradiation, the diazo peaks dropped 60% and the acid peaks grew to 150% of the original value.

In contrast, samples that were irradiated in air with X-rays to doses of 500 mJ/cm^2 and 2500 mJ/cm^2 showed a different behavior. While the peaks corresponding to the diazo starting material showed decreases of 22% and 54%, respectively, there was no evidence of formation of the acidic photoproduct, even at the high dose. This result indicates a clear difference in chemistry between X-ray and optically exposed samples. Since formation of the

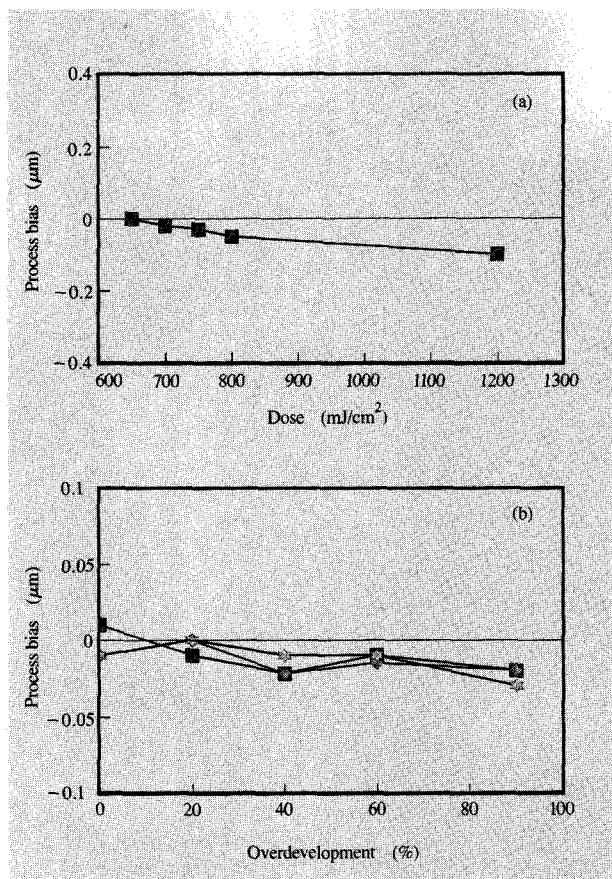


Figure 3

Effect on linewidth of (a) changes in exposure dose and (b) development time for TNS resist.

carboxylic product is assumed to be partially responsible for the lithographic dissolution rate difference between exposed and unexposed resist in optical lithography, a different conversion must be occurring in X-ray lithography. While we did not do a detailed product analysis in this experiment, these results are qualitatively similar to results seen in e-beam lithography [6]. In this case, product analysis indicates that e-beam-irradiated samples do not show any evidence of carboxylic acid formation but do show formation of naphtholic-type products which would be expected to dissolve in developers, thereby accounting for the lithographic activity.

Concerns about the limited sensitivity of diazoquinone novolak resist have driven the investigation of chemically amplified resists [8] for X-ray applications. **Figure 2(b)** is a schematic of a positive-working, chemically amplified resist. In this material, a photogenerated catalyst, commonly a strong acid, is formed in the exposed areas.

Following exposure, a bake step is performed to speed along a chemical change catalyzed by the acid. In this way, one chemical change that takes place during the exposure step can be transformed into numerous chemical events during the subsequent bake step, thus amplifying the effect of the exposure. In this case, the acid-catalyzed decomposition of the t-butyloxycarbonyl (tBOC) protecting group liberates the phenolic hydroxyl functionality, which is soluble in the basic developer. Obviously, controlling the kinetics during the bake step now becomes critical. Also, complications from undesired quenching of the catalyst from airborne contaminants can destroy the lithographic imaging capability of this type of material.

A negative chemically amplified resist is similar in principle. In this case, however, the acid-catalyzed chemistry is typically a cross-linking reaction. This increases the molecular weight of the material and effectively makes it a solid cross-linked network. The lithographic activity results from the fact that this network is no longer soluble in the developer, as was the original resin. A negative-tone image then results, since the resist that was originally exposed now remains after development.

Lithography of resist materials under synchrotron irradiation

As in other lithographies, the key in X-ray lithography is to control the linewidth of critical features as precisely and accurately as possible. In X-ray lithography, the ability to control linewidth is greater than in conventional optical lithography. X-rays are less subject to diffraction effects, since the wavelength is much shorter; as a result, the aerial image more closely resembles the mask. The resist therefore "receives" an image with much sharper and more clearly defined edges, making it easier to replicate the mask. However, the ability to control linewidth is heavily dependent on the ability of the resist to convert this imaging information into a resist stencil. It is therefore important to understand the process variables that affect a resist's response to image information.

One's ability to maintain good linewidth control (LWC) can be estimated if one knows how the feature size depends on processing variables. This is often referred to as the process latitude of a given resist process. Some of the key process variables include the postapply bake (PAB) time and temperature, exposure dose, postexposure bake (PEB) time and temperature (this is particularly important for chemically amplified resist systems), and development effects. Virtually every step of the resist process can be characterized, and with each step a latitude can be defined (e.g., exposure latitude, PEB latitude). Typically the latitude is defined as the change in linewidth with respect to a given change in a process variable. As described herein, if the process latitude with respect

to each of these variables of a resist system is well characterized, one can quantitatively predict the linewidth control one observes on a given set of wafers.

Another characteristic of a resist is the "contrast" of the resist system as defined by gamma, which is the linear part of the curve of normalized resist thickness vs. log (dose) as the thickness goes to zero. This curve is typically referred to as a contrast curve (see Figure 8, shown later, as an example). As is described later in this section, this parameter, while often used to characterize a resist, may not be very indicative of the type of linewidth control one might expect from a resist system.

The classical materials used for X-ray lithography are similar to those used in other lithographies in their infancy, e.g., polymethyl methacrylate and related materials [9]. While these are high-resolution materials, lack of compatibility with other semiconductor processes and poor sensitivity have limited their use in device fabrication.

The first fully scaled 0.5- μm CMOS circuits fabricated wholly by synchrotron XRL were made with conventional optical resist materials [10]. A diazoquinone novolak i-line resist, TNS, was used for the positive-tone levels, and a negative-tone cross-linking resist, Hitachi RD2000N, was used on other levels. The focus of this study was on process latitude and repeatability of linewidth across the wafers. The effects of development time and exposure dose are shown in Figure 3. Note that even large changes in processing conditions result in only modest changes in linewidth. The effects of this relatively flat response with respect to process are reflected in the linewidth repeatability results shown in Figure 4. Included in these results is the noise of the measurement technique, which is estimated to be 50–70 nm.

More recently, chemically amplified resists have been investigated for use in X-ray lithography. Several materials were investigated and compared to the novolak resist described above [11]. These materials were processed under nominal operating points with standard processes that were not optimized for XRL, and these data were taken on flat silicon substrates. The materials investigated were APEX, a commercially available positive-tone system, and two IBM experimental negative-tone epoxy-type cross-linking resists, ER-1 and ER-2. Shown in Table 1 are 1σ repeatability measurements for APEX and two experimental negative-tone systems, along with the breakdown of these numbers into various components. The components are across-field variation, wafer-to-wafer variation, and across-wafer variation. APEX showed results comparable to those for the novolak resist, but the other experimental materials were significantly worse.

In looking at Table 1 it is apparent that the major contributor to loss of linewidth control in ER-1 and ER-2 is across-field nonuniformity. Further analysis has indicated that this is due to a nonuniformity in dose across

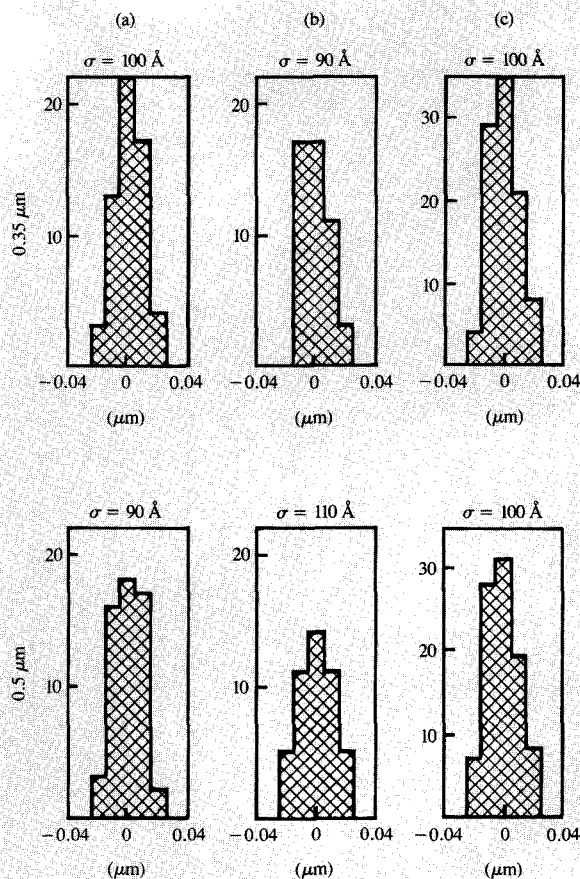


Figure 4

Field-to-field linewidth variation (1σ in μm) for TNS resist (a) within wafer, (b) wafer to wafer, (c) total, for nominal linewidths of 0.35 and 0.5 μm .

Table 1 Linewidth variation (1σ values in μm) for APEX resist and two experimental resist systems (ER-1, ER-2) compared to TNS (novolak) resist.

Resist	Exposure (mJ/cm^2)	1σ linewidth variation (μm)			
		Raw data	Across- field	Wafer- to-wafer	Across- wafer
Novolak	750	0.010	0.008	0.009	0.008
APEX	60	0.009	0.008	0.007	—
ER-1	15	0.076	0.063	—	0.020
ER-2	16	—	0.046	—	—
	23	0.035	0.035	0.015	—
	29	0.049	0.047	0.022	—
	35	0.123	0.117	0.047	—

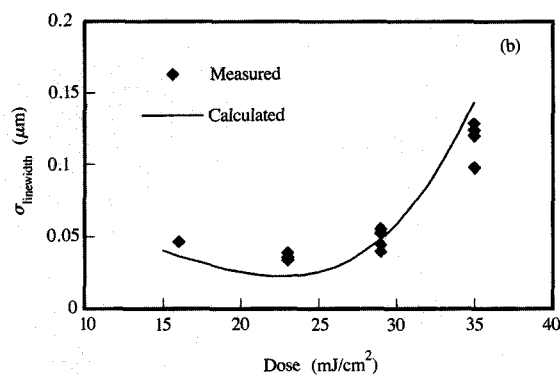
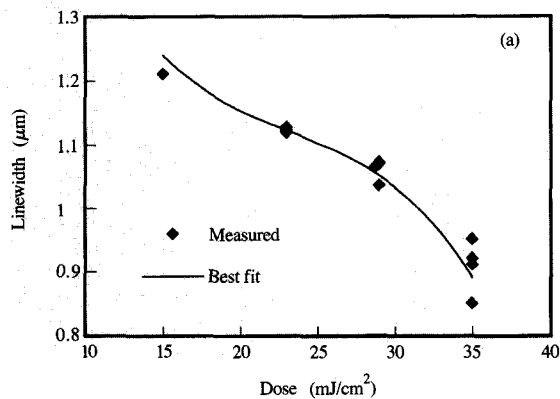


Figure 5

(a) Exposure latitude of ER-2 resist expressed as linewidth variation vs. dose; (b) calculated and experimental across-field linewidth variance for ER-2.

the field. This result suggests that these experimental materials have inherently poor exposure latitude. This was measured; **Figure 5(a)** demonstrates the large changes in linewidth as a result of changes in dose.

Knowing the linewidth change as a function of dose and the dose variation across the field, one can calculate the overall variation in linewidth across the field. The results of this calculation as a function of dose are shown in **Figure 5(b)** and are compared to the experimentally measured values. The agreement between these indicates that the majority of loss of linewidth control for this system is primarily a result of the dose nonuniformity across the field, since it was the only variable assumed in the calculation. It is interesting to note that there is a minimum in the curve in **Figure 5(b)**, indicating that there is an optimal dose at which one would like to operate for this resist system. At either lower or higher doses, the linewidth control degrades. Also of interest is the fact that

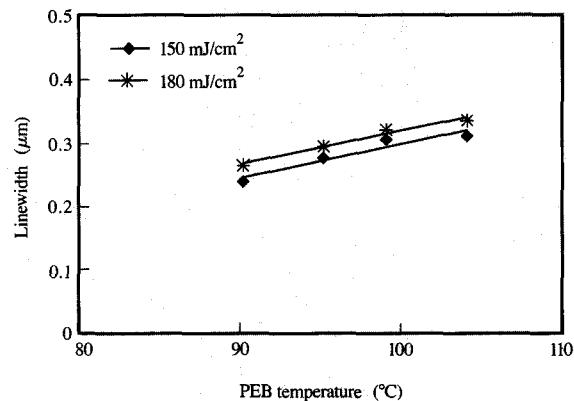


Figure 6

Effect of postexposure bake on linewidth for a negative-tone chemically amplified resist, CGR.

APEX was able to deal with the dose nonuniformity better because of its vastly superior exposure latitude. Although the dose latitude of the ER systems is insufficient for good lithography, they served as excellent test cases and demonstrated that one can calculate the linewidth control that would be expected if one knows the important variables to a sufficient degree.

For chemically amplified resists, one of the most important parameters to control is the kinetics of the postexposure bake (PEB). During this step the lithographically important chemistry takes place, and since it is a catalytic reaction, careful control of the process conditions must be maintained in order to achieve consistent results. A negative chemically amplified system, CGR, was recently reported that demonstrates relatively stable linewidth control with respect to PEB [12]. **Figure 6** shows the change in linewidth as a function of PEB temperature. This corresponds to 5 nm change in linewidth per degree centigrade, which is $\sim 5\times$ better than other chemically amplified resists reported in the literature [13]. This resist also showed the capability for high-resolution imaging, as shown in **Figure 7**.

Effect of dissolution properties on lithography

In order to understand and optimize lithographic performance for resist systems under synchrotron irradiation, simulations were performed.* For this study, we used the results from aerial image calculation from XMAS [14] and the string model from SAMPLE [15] to calculate resist profiles and final linewidths.

*W. Conley and D. Seeger, 1991, unpublished results.

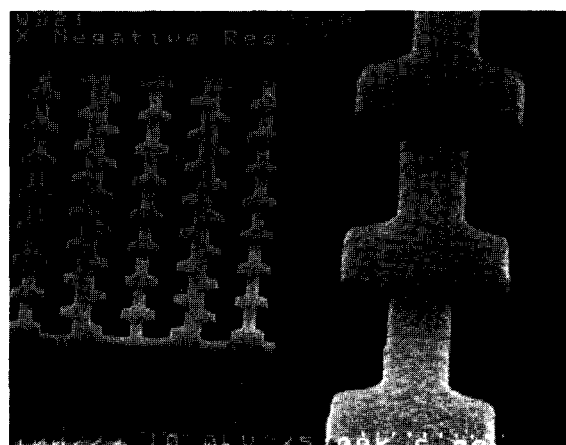
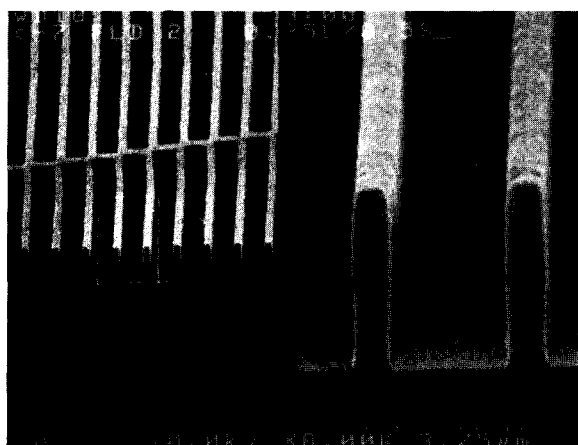
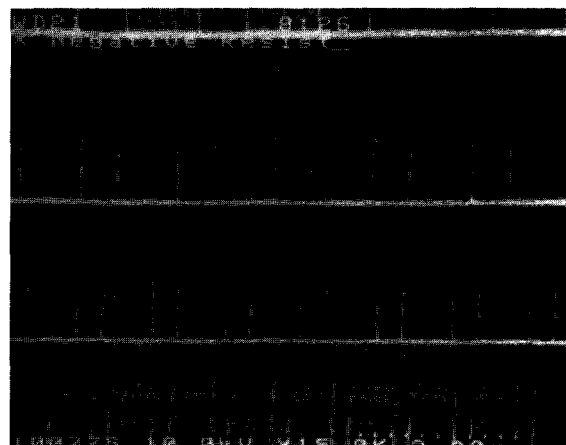
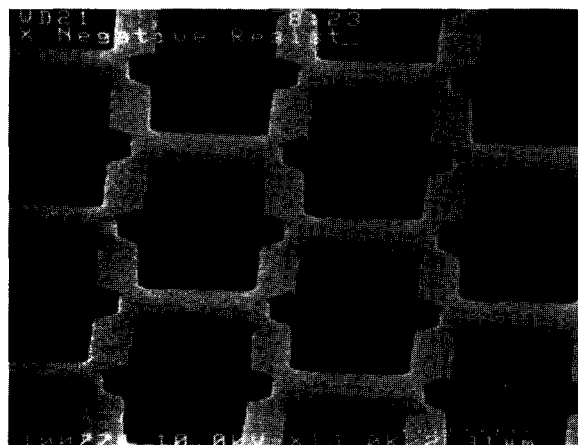
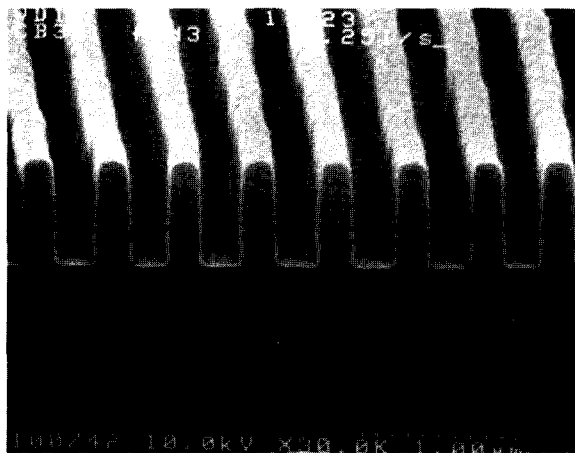


Figure 7

High-resolution images in CGR resist exposed at 150 mJ/cm².

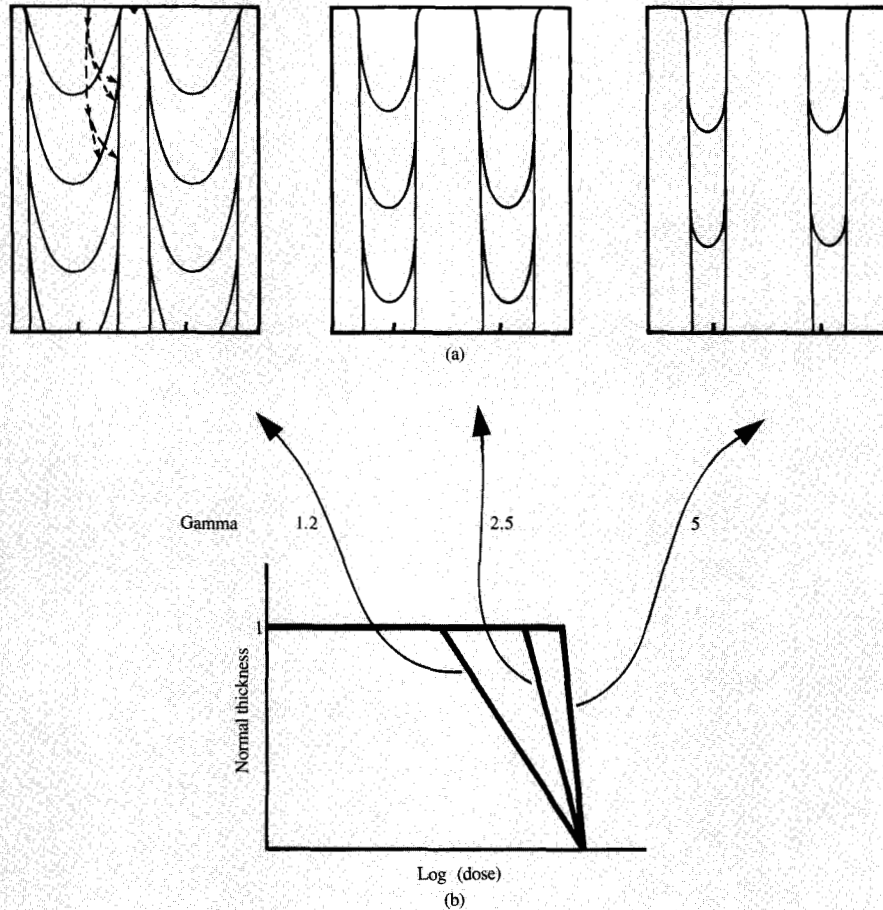


Figure 8

Effect of varying gamma (contrast) on profiles for theoretical resists. Resist profiles for equal line/space patterns are shown for three values of gamma in (a) for 30-s development time intervals, while the contrast for these gamma values is shown in (b).

In order to verify the model, dissolution rates from TNS were determined empirically as a function of X-ray exposure dose, and the best fit from the results was utilized. Resist profiles calculated using this model are vertical in agreement with empirical results. The simulation also shows quantitative agreement with experiment for both dose and development latitude, further indicating the validity of the model.

A set of contrast curves for various "theoretical" or idealized resists were used in order to determine the effect on lithographic characteristics. For these simulations, a 0.25- μm line/space pattern with a 0.6- μm -thick gold absorber on silicon membrane at a 40- μm gap was assumed. It is also assumed that the source is spatially coherent (i.e., no penumbral blur) and the resist sensitivity

is 100 J/cm³. The same aerial image (0.25- μm lines/spaces) was used for all of these calculations. In order to look at effects of changes in dissolution properties in the resist, the contrast curve is varied. For all calculations, we assume that there are finite regions along the dose axis of the contrast curve, with each region having a discrete linear dissolution rate. A change in the contrast curve results in a change in the dissolution rates in these regions. These dissolution rates are then used in the model. A "breakpoint" is defined as any point along the contrast curve where the slope of the line changes.

The first set of contrast curves used for the calculations are shown in **Figure 8**, in which the only parameter that is changed is gamma (commonly referred to as "contrast"). The resist profiles are shown as several contours, each

contour representing the results after an additional 30 seconds of development. Surprisingly, resist profiles are vertical, independent of contrast.

Since this result seemed counterintuitive, experimental verification was pursued. A resist with poor X-ray contrast, Shipley PL-1, was purposely chosen. Note that this material was not designed for high-resolution lithography, which explains its low contrast. Its X-ray contrast was measured as 1.3. As a reference, contrast values in excess of 3–4 are generally believed to be necessary in optical lithography for good imaging. Nonetheless, we were able to achieve vertical profiles, as shown in **Figure 9**. This is partially a function of the low absorption of organic resist at these wavelengths.

However, examination of the behavior of the calculation warrants further consideration. If we choose an imaginary point along the resist surface near the edge of a resist feature, when development begins this point initially moves toward the wafer surface (see **Figure 8**, upper left). As development proceeds, this point begins to move toward the resist edge until it finally stops at that edge. From that time on, the point does not move, regardless of how long development proceeds, because at that point the rate of dissolution has been defined to be zero (at the point in resist that receives a dose less than or equal to the breakpoint dose). As a result, the profile is vertical, since all such points along the edge of the resist hit this “wall” where no further development occurs. Further development does not change the linewidth, and such a resist system has infinite development latitude. Of course, real resist systems do not behave this way, showing some finite development rate and some degradation of wall profile (see below). The important point here is that contrast as defined by gamma is *not* what is controlling the wall profile. What is controlling the profile appears to be the “sharpness” of the breakpoint.

The other effect with increasing contrast is related to linewidth. Higher-contrast resist results in wider resist lines under the same dose and development conditions. This result of the calculation is explained by noting that with increasing contrast, the breakpoint for these resists changes (moves higher in dose with increasing contrast; see bottom of **Figure 8**). If the breakpoint dose is defined in this case as the minimum dose at which there is an onset of dissolution, the resist acts like a “thresholding” resist. That is, at all doses above the breakpoint dose, the resist develops to the wafer surface; below that dose, there is no development. Since this breakpoint changes with contrast, the area in the resist that receives this dose is different, resulting in a different linewidth. The factor that controls the distribution of dose in the resist film is defined by the aerial image used in the calculation.

Figure 10 shows the effect of resist thinning on profiles. As expected, the thinner the resist, the worse the profiles.

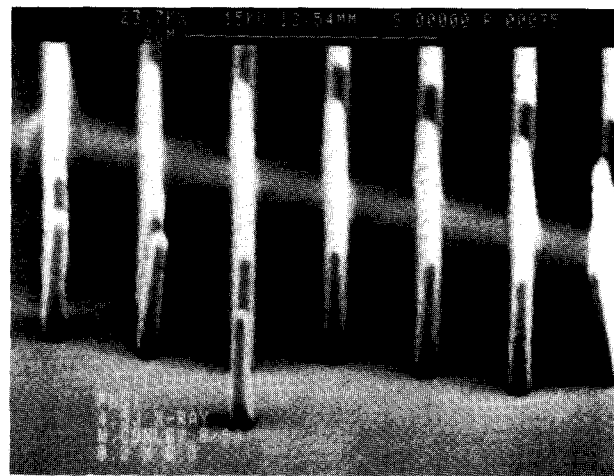
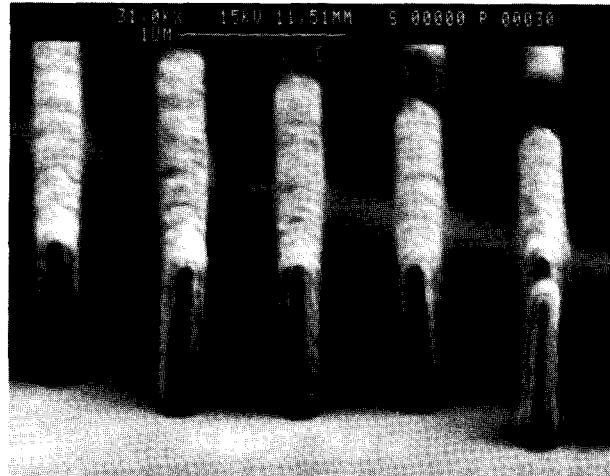


Figure 9

Scanning electron micrographs of profiles from X-ray-exposed Shipley PL-1 resist.

This result was experimentally verified by changing the PL-1 process to intentionally allow 1000 Å of thinning (**Figure 11**). Note the tapered profiles. We also examined the effect of thinning on dose and development latitude. Interestingly, more thinning does not affect dose latitude, and, as expected, thinning reduces development latitude.

Finally, we used the contrast curves shown in **Figure 12**, where a rounding at the breakpoint dose is simulated. This is done by putting in a “shoulder” incorporating two breakpoint doses (one dose higher than the other). The profiles thus obtained show more sloping of the images, which is more characteristic of a real resist system. Increasing the higher breakpoint dose has no significant effect on profiles. This is as expected, since at the limit where the upper breakpoint dose increases until it crosses

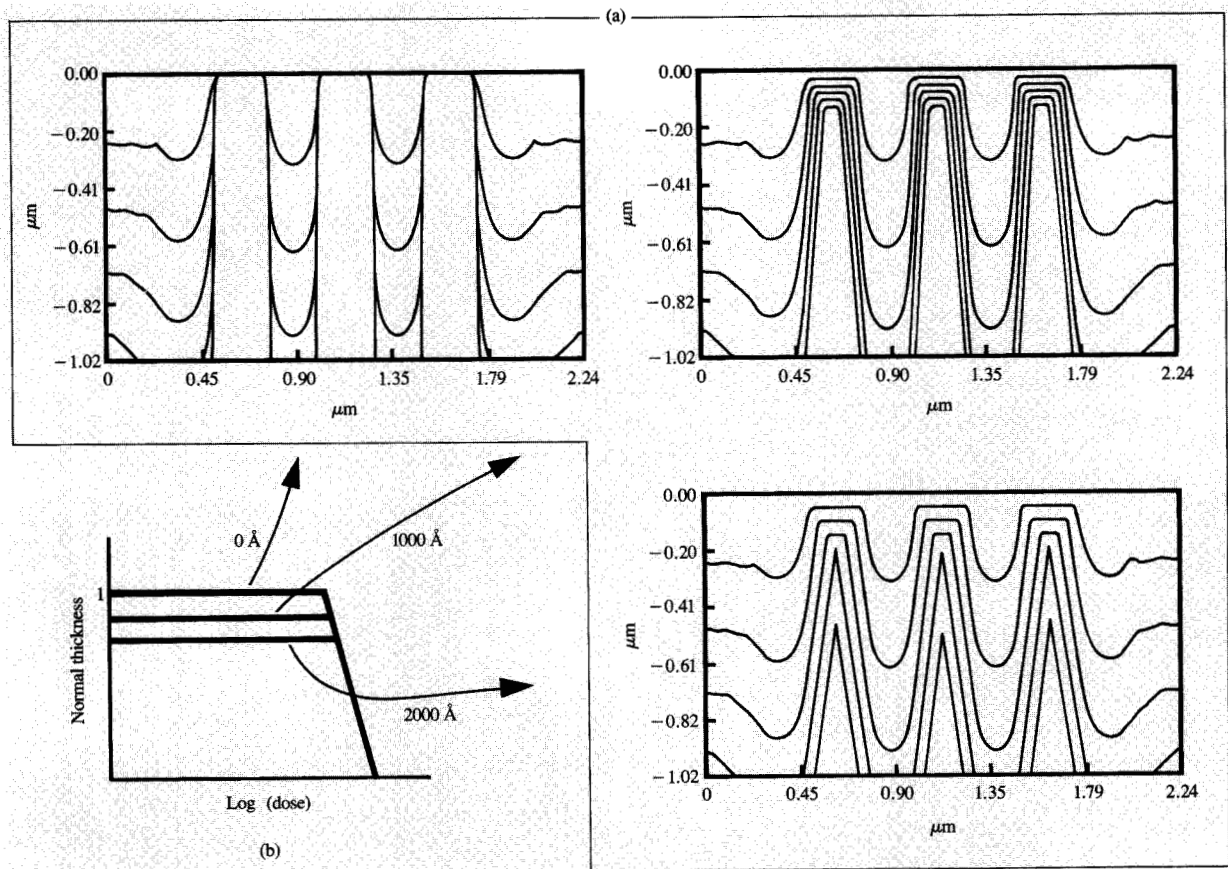


Figure 10

Effect of resist thinning on profiles as calculated for a theoretical series of resists. Resist profiles for equal line/space patterns are shown for three values of resist thinning in (a) for 30-s development time intervals, while the thickness as a function of dose is shown in (b).

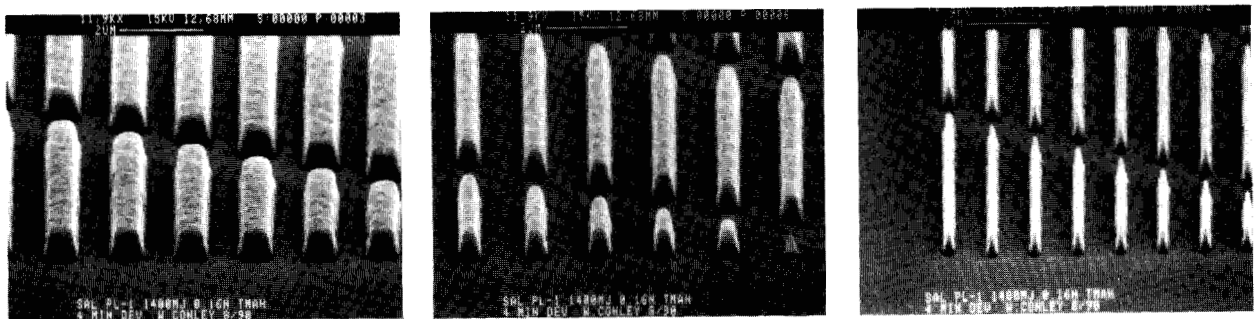


Figure 11

Scanning electron micrographs of Shipley PL-1 resist processed to include intentional thinning during development.

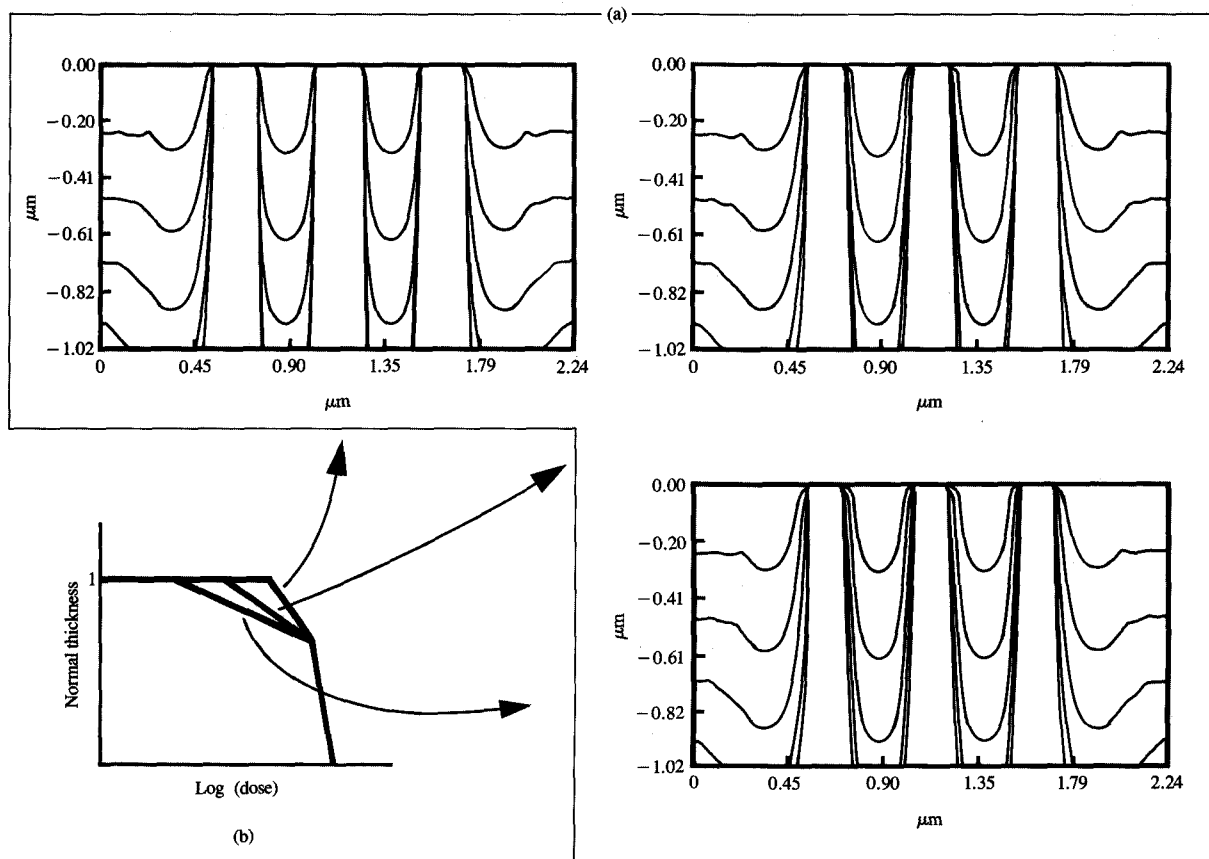


Figure 12

Effect of changing contrast curve on a series of theoretical resists. Resist profiles for equal line/space patterns are shown for three different contrast curves in (a) for 30-s development time intervals, while the assumed contrast curves are shown in (b).

the x -axis, the effect is similar to varying gamma only, which, as described above, has no effect on profiles.

Figure 12 shows that by lowering the lower breakpoint dose, the profiles are degraded. This is also as expected, since if one continues to lower the dose, it approaches a contrast curve of a resist that thins and therefore degrades profiles (see earlier discussion).

Thus, gamma is a poor way to characterize resist for X-ray lithography. More subtle effects in the contrast curve (e.g., shoulders) can have a significant impact on profiles and process latitude.

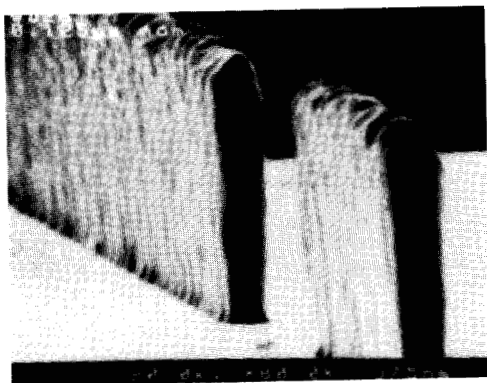
Extendibility of X-ray resist materials

One of the perceived advantages of XRL is the relative ease of extending the lithography to smaller feature sizes. Figure 13 shows different isolated resist images from 1 μm down to 0.125 μm , and Figure 14 shows the effect on image size of changing exposure and mask-to-wafer gap

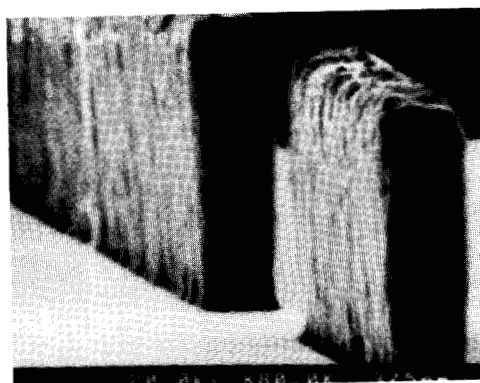
[16]. Notice again that the linewidth is relatively independent of mask-to-wafer gap, and notice also the large distance between the lines at the top of the plot (+10% of nominal critical dimension) and those at the bottom (-10% of nominal critical dimension). This is indicative of a large exposure latitude even at these fine feature sizes. The stability of linewidth under identical processing conditions over time has also been demonstrated for very high-resolution features. For 0.2- μm isolated resist lines, field-to-field repeatability was measured and found to be ~ 30 nm (3σ) [16]. These data were collected from two separate X-ray steppers on the same process line over a four-month period by sampling wafers from a variety of wafer lots.

Though this appears to demonstrate the capability of XRL, it should be noted that at these small dimensions and large aspect ratios, materials issues become important. At higher aspect ratios, resist lines begin to fall over,

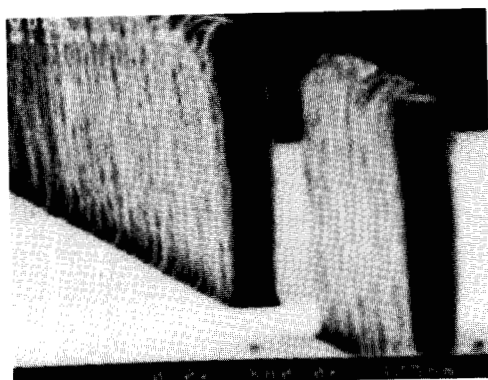
0.125 μm



0.25 μm



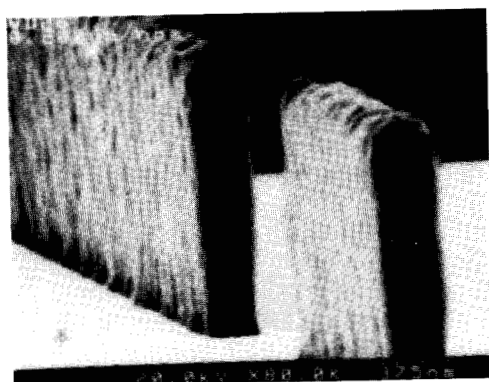
0.150 μm



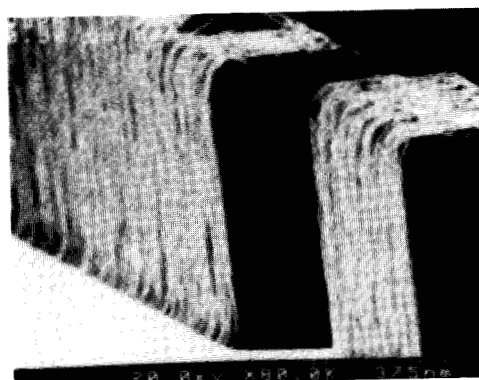
0.35 μm



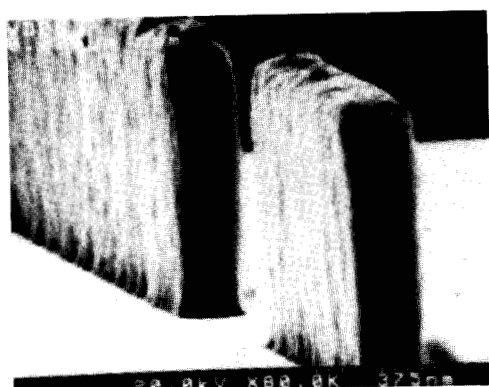
0.20 μm



0.5 μm



0.225 μm



1.0 μm



Figure 13

Resist profiles from APEX exposed at 40- μm mask-to-wafer gap with a dose of 75 mJ/cm^2 .

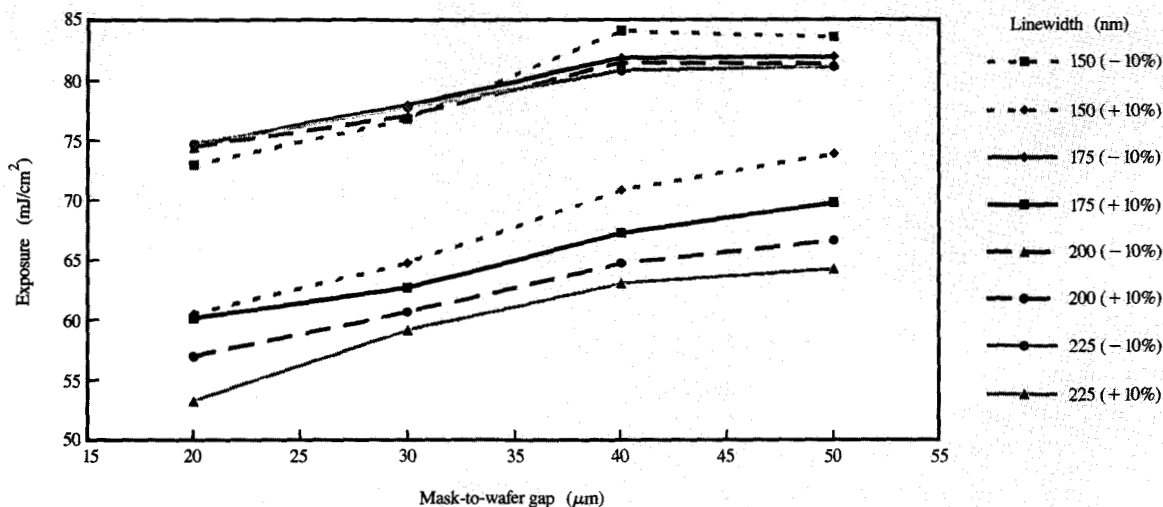


Figure 14

Effect on linewidth of changing exposure dose and mask-to-wafer gap for an isolated resist feature in APEX resist. This figure shows the locus of $\pm 10\%$ change in nominal width of features of four different widths.

presumably because of limitations in the mechanical strength of the material. Also, the mechanical action of the development process itself can destroy the integrity of the resist image at these small dimensions.

To realize the potential of XRL, continued emphasis must be placed on materials improvements. These improvements must be studied in conjunction with other aspects of the semiconductor process. If, for example, one improves the etch resistance of a resist material, a thinner layer of resist can be used as the etch mask, thereby reducing the requirement on mechanical stability.

The other improvements that will need investigation concern the manufacturability of resist processes. In order to take advantage of a stable X-ray exposure process, resist processes of stability equal to or better than current ones will be needed. This includes stability with respect to all processing conditions, including baking of the resist, development processes, and resistance to contamination from the substrate and/or environment. By developing these types of stable resist systems, extension of XRL to even smaller dimensions can be realized.

Acknowledgments

The author gratefully acknowledges all of the contributors to this work, including co-authors in the cited references as well as the staff of the IBM ALF facility in East Fishkill, New York. I would also like to thank Don Hofer for the many useful suggestions he made to improve this paper.

References

1. K. Valiev, *The Physics of Submicron Lithography*, Plenum Press, New York, 1992; *Radiation Chemistry: Principles and Practices*, Farhatziz and M. Rodgers, Eds., VCH Publications, New York, 1987.
2. G. Taylor, "X-ray Resist Materials," *Solid State Technol.* **23**, 73 (1980); J. Greeneich, "X-ray Lithography: Part I—Design Criteria for Optimizing Resist Energy Absorption; Part II—Pattern Replication with Polymer Masks," *IEEE Trans. Electron Devices* **ED-22**, 434 (1975).
3. E. Eranian, A. Coutlet, E. Datamanti, and J. DuBois, "Halogenated Polymethacrylates for X-Ray Lithography," *Amer. Chem. Soc. Symp. Ser.* **151**, 275 (1981).
4. W. Moreau, *Semiconductor Lithography: Principles, Practices, and Materials*, Plenum Press, New York, 1988, p. 111.
5. (a) J. Choi, J. Moore, J. Corelli, J. Silverman, and H. Bakhru, "Degradation of Poly(methylmethacrylate) by Deep Ultraviolet, X-Ray, Electron Beam, and Proton Beam Irradiations," *J. Vac. Sci. Technol. B* **6**, 2286 (1988).
6. J. Pacansky and R. Waltman, "Solid-State Electron Beam Chemistry of Mixtures of Diazoketones in Phenolic Resins: AZ Resists," *J. Phys. Chem.* **92**, 4558 (1988).
7. J. Pacansky and J. R. Lyster, "Photochemical Decomposition Mechanisms for AZ-Type Photoresists," *IBM J. Res. Develop.* **21**, 42 (1979).
8. C. Willson, H. Ito, and J. Frechet, "A Sensitive Deep UV Resist System," Society of Plastics Engineers Regional Technical Conference on Photopolymers: Principles, Processes, and Materials, Ellenville, NY, Nov. 8–10, 1982.
9. I. Haller, R. Feder, M. Hatzakis, and E. Spiller, "Copolymers of Methyl-Methacrylate and Methacrylic Acid and Their Metal Salts as Radiation Sensitive Resists," *J. Electrochem. Soc.* **126**, 154 (1979).
10. D. Seeger, K. Kwietniak, D. Crockatt, A. Wilson, and J. Warlaumont, "Fabrication of 0.5 μm CMOS Devices by

Synchrotron X-Ray Lithography: Resist Materials and Processes," *Microelectron. Eng.* **9**, 97 (1989).

11. D. Seeger, R. Wood, J. Gelorme, and K. Stewart, "Linewidth Control in Sensitive X-Ray Resist Systems," *Proceedings KTI Microelectronics Seminar—Interface '89*, San Diego, November 6–7, 1989, p. 351.
12. D. Seeger, R. Viswanathan, C. Blair, J. Gelorme, and W. Conley, "Single Layer Chemically Amplified Resist Processes for Device Fabrication by X-Ray Lithography," *J. Vac. Sci. Technol. B* **10**, 2620 (1992).
13. D. Seligson, S. Das, and H. Gaw, "Process Control with Chemical Amplification Resists Using Deep Ultraviolet and X-Ray Radiation," *J. Vac. Sci. Technol. B* **6**, 2303 (1988).
14. H. Oertel, M. Wess, H. Huber, Y. Vladimírsky, and J. Maldonado, "Modeling of Illumination Effects on Resist Profiles in X-ray Lithography," *Proc. SPIE* **1465**, 244 (1991).
15. K. Toh and A. Neuruether, "Three Dimensional Simulation of Optical Lithography," *Proc. SPIE* **1463**, 356 (1991).
16. A. Pomerene, D. Seeger, and P. Blauner, "Photoresist Process Latitude Optimization for Synchrotron X-Ray Lithography," *Proceedings of the International Society for Optical Engineering Symposium on Microlithography*, Santa Clara, CA, March 1993, in press.

Received December 29, 1992; accepted for publication
May 14, 1993

David Seeger IBM Research Division, Thomas J. Watson Research Center, P.O. Box 218, Yorktown Heights, New York 10598 (SEEGER at YKTVMV). Dr. Seeger joined IBM in 1983 after receiving his Ph.D. in physical-organic chemistry from Yale University. He has been involved in development of materials and processes for optical, X-ray, and e-beam lithography. His primary focus over this time has been in X-ray lithography examining advanced processes for X-ray printing as well as patterning of X-ray masks. Dr. Seeger is currently manager of an advanced materials and process group responsible for the development of both X-ray and advanced optical resist processes.